2006

The hydrodynamic effects of shape and size change during reconfiguration of a flexible macroalga

Michael L. Boller
University of Rhode Island

Emily Carrington
University of Rhode Island

Citation/Publisher Attribution
Boller, M. L., & Carrington, E. (2006). The hydrodynamic effects of shape and size change during reconfiguration of a flexible macroalga. *Journal of Experimental Biology, 209,* 1894-1903. doi: 10.1242/jeb.02225
Available at: https://doi.org/10.1242/jeb.02225

The Journal of Experimental Biology 209, 1894-1903
Published by The Company of Biologists 2006
doi:10.1242/jeb.02225

The hydrodynamic effects of shape and size change during reconfiguration of a flexible macroalga

Michael L. Boller* and Emily Carrington†

Department of Biological Sciences, University of Rhode Island, Kingston, RI 02881, USA

*Author for correspondence at present address: Hopkins Marine Station of Stanford University, Pacific Grove, CA 93950, USA (e-mail: boller@stanford.edu)

†Present address: Department of Biology, University of Washington, Friday Harbor Laboratories, Friday Harbor, WA 98250, USA

Accepted 21 March 2006

Summary

Rocky intertidal organisms experience large hydrodynamic forces due to high water velocities created by breaking waves. Flexible organisms, like macroalgae, often experience lower drag than rigid organisms because their shape and size change as velocity increases. This phenomenon, known as reconfiguration, has been previously quantified as Vogel's *E*, a measure of the relationship between velocity and drag. While this method is very useful for comparing reconfiguration among organisms it does not address the mechanisms of reconfiguration, and its application to predicting drag is problematic. The purpose of this study was twofold: (1) to examine the mechanisms of reconfiguration by quantifying the change in shape and size of a macroalga in flow and (2) to build a mechanistic model of drag for reconfiguring organisms. Drag, frontal area and shape of the intertidal alga *Chondrus crispus* were measured simultaneously in a recirculating flume at water velocities from 0 to ~2 m s^{-1}. Reconfiguration was due to two separate mechanisms: whole-alga realignment (deflection of the stipe) at low velocities (<0.2 m s^{-1}) and compaction of the crown (reduction in frontal area and change in shape) at higher velocities. Change in frontal area contributed more to drag reduction than change in drag coefficient. Drag coefficient and frontal area both decrease exponentially with increasing water velocity, and a mechanistic model of drag was developed with explicit functions to describe these changes. The model not only provides mechanistic parameters with which to compare reconfiguration among individuals and species, but also allows for more reliable predictions of drag at high, ecologically relevant water velocities.

Key words: biomechanics, ecology, seaweed, *Chondrus crispus.*

Introduction

The distribution and abundance of rocky shore intertidal organisms are partly determined by damage and dislodgement caused by the hydrodynamic forces created by breaking waves (Dayton, 1971; Menge, 1976; Paine and Levin, 1981; Denny, 1995; Carrington, 2002). These forces include the well-known lift and drag, and also the impingement force, associated with the impact of a wave on an emerged object (Gaylord, 2000). Sessile organisms have adopted a variety of different strategies for surviving these physical stressors (Denny et al., 1985). Some, such as limpets and sea stars, are rigid and armored while others, such as anemones and macroalgae, are flexible (Koehl, 1977; Vogel, 1994; Denny, 1988). The dominant hydrodynamic force imposed on macroalgae is likely drag (Denny and Gaylord, 2002). The impingement force may often exceed drag in the intertidal zone (Gaylord, 2000), but has not been extensively studied and is not addressed here.

For macroalgae, two mechanisms have been identified by which marine macroalgae use flexibility to reduce drag. First, this hydrodynamic force may be decreased in macroalgae by 'going with the flow' and reducing the velocity of the water relative to their blades (Koehl, 1984; Koehl, 1986; Koehl, 1999; Gaylord and Denny, 1997; Denny et al., 1997; Stewart, 2004). A second mechanism is called reconfiguration, where the size and shape of the macroalga changes with velocity to reduce drag (Vogel, 1984; Vogel, 1989; Sheath and Hambrook, 1988; Carrington, 1990; Gaylord and Denny, 1997; Johnson, 2001; Pratt and Johnson, 2002; Sand-Jensen, 2003; Harder et al., 2004). For macroalgae, the reduction in drag *via* reconfiguration is due to a passive bending of the organism in response to the force (Vogel, 1994).

In general, biologists define drag (F_D) as:

$$F_D = \tfrac{1}{2}\rho U^2 A C_D , \quad (1)$$

where ρ is the density of the fluid, U is the fluid velocity relative to the organism, A is a characteristic area (size) of the organism, and C_D is the drag coefficient, a dimensionless number that accounts for the interaction between the flow and the shape of

the object. In this equation, reconfiguration is not addressed because the size and shape of the organism are assumed to be constant. However, the relationship between drag and reconfiguration has been quantified as Vogel's E, a measure of the difference between the squared relationship between velocity and drag and the lower drag seen in reconfiguring organisms (Vogel, 1994). Vogel's E is easily calculated as the slope of the linear regression of the log–log plot of speed-specific drag (F/U^2) *versus* fluid velocity (U). Values for Vogel's E typically range from 0 to –2; more negative values imply increased reconfiguration. Reconfiguration has been incorporated into Eqn 1 by modifying the exponent of velocity by subtracting Vogel's E, resulting in the equation:

$$F_D = \tfrac{1}{2}\rho U^{2-E} A_{plan} C_D , \quad (2)$$

where A_{plan} is the planform area. This basic equation is reported in different forms (Denny, 1995; Gaylord, 2000; Denny and Gaylord, 2002).

While Vogel's E is useful for quantifying reconfiguration and comparing drag among organisms, its application is limited. First, it is an indirect measure of reconfiguration. While it is the shape and size that change with increasing water velocity, Vogel's E modifies the exponent of the velocity only. Direct measurements of changes in shape and area should be considered independently to understand the mechanisms of reconfiguration. Second, the introduction of Vogel's E to the exponent of velocity modifies the dimensionality of C_D (Denny and Wethey, 2001; Sukhodolov, 2005) (but see Sand-Jensen, 2005), which was originally defined as a unitless parameter (Vogel, 1994). Thus, drag coefficients calculated for organisms with different Vogel's E have different units, complicating their comparison. Third, Vogel's E characterizes reconfiguration over the range of velocities for which it is measured. It should not used to extrapolate drag at higher velocities, despite its use for such a purpose in the literature (Vogel, 1994).

While it is commonly accepted that reconfiguration can be of great importance for reducing drag on macroalgae (Denny and Gaylord, 2002; Harder et al., 2004), the mechanisms of reconfiguration, specifically how changes in area and shape combine to reduce drag and the relative contributions of each mechanism to the overall reconfiguration, are poorly understood. This study examined reconfiguration of the red alga *Chondrus crispus*, a dominant space holder in the New England rocky intertidal zone, to determine the mechanisms of drag reduction *via* flexibility. The changes in algal size and shape in flow were measured directly, allowing for a comparison of their contributions to drag reduction. Further, these analyses allow for the development of a new mechanistic model for drag on flexible organisms.

Materials and methods

Algal collection

Nineteen undamaged and non-reproductive *Chondrus crispus* Stackhouse were collected from sites in the lower intertidal zone at Black Point and Bass Rock in Narragansett, Rhode Island, USA (41.40°N, 71.45°W and 41.39°N, 71.47°W, respectively). Individual algae were selected to span a range of morphologies (small to large crown areas) and were collected undamaged by removing the rock underlying the holdfast with a hammer and chisel. The algae were brought to the lab and maintained in ~17°C seawater for up to 3 days. The holdfast of each individual was carefully dissected from the rock and shaved with a razor blade to achieve a flat surface that was then affixed to an acrylic mount using cyanoacrylate glue. Life history phase was identified after hydrodynamic analyses using a resorcinol test (Garbary and DeWreede, 1988) and only gametophytes were used in the study. The height (±0.02 cm) and planform area A_{plan} (±0.0004 cm^2) were measured using ImageJ software (ver. 1.33, National Institutes of Health, Bethesda, MD, USA) from photographs of individuals sandwiched between two sheets of acrylic.

Hydrodynamic characterization

The hydrodynamic performance of each individual was measured in seawater using a medium-speed recirculating flume similar to those described by Denny (Denny, 1988), but modified for direct measurement of reconfiguration (Fig. 1). The flume consisted of a rectangular acrylic outer tank above a PVC return pipe (~0.2 m diameter, 0.031 m^2 cross-sectional area), supported by a custom-designed extruded aluminum frame (80/20 Inc., Columbia City, IN, USA). Within the rectangular tank, a choke reduced the cross-sectional area to 0.0225 m^2 in the 0.15 m×0.15 m×0.30 m (W×H×L) working section. A diffuser gradually increased the cross-sectional area downstream of the working section. Turning vanes mounted within each elbow of the return pipe and two sets of flow straighteners (0.013 m square, 0.00016 m thick plastic grid) stabilized the flow. Flow was generated by two

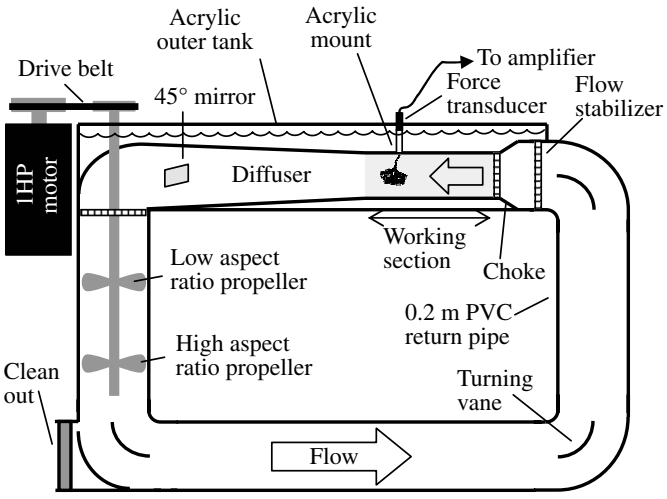

Fig. 1. Recirculating flow tank with modifications for direct measurement of reconfiguration. The overall length of the tank was 2.4 m; the working section was 0.15 m×0.15 m×0.30 m (W×H×L). Algae (in the working section) were inverted to keep the force transducer dry. The 45° mirror allowed for the visualization of the frontal area of the alga as it reconfigured in flow.

19 cm bronze propellers driven by a 1 HP variable speed DC permanent magnet motor (PM9100TF, Boston Gear, Quincy, MA, USA). The motor controller (RG500A, Minarik Corp., Glendale, CA, USA) was interfaced with the analog output of an analog-to-digital converter (DAS16/12-AO, Measurement Computing Corp., Middleboro, MA, USA), allowing water velocity to be controlled by the data collection computer. Water velocity (±0.2 m s^{-1}) was calibrated to propeller speed (r.p.m.) by following neutrally buoyant particles with a high-speed digital video system (Motionscope PCI, Redlake, San Diego, CA, USA). Hydrodynamic performance variables (i.e. drag, area, shape) were recorded across velocities ranging from 0 to ~2 m s^{-1} at ~0.1 m s^{-1} intervals.

Drag (±0.001 N) was measured on each individual using a 1 kg (9.8 N) strain gage force transducer (FORT1000, WPI Inc., Sarasota, FL, USA). An aluminum adapter connected the force transducer to the acrylic mount and extended the moment arm to 10 cm. This extension decreased the maximum load to ~2 N but increasing the sensitivity of the transducer. The force signal was amplified by a transducer amplifier (TBM4, WPI Inc.) and calibrated by hanging weights from the acrylic mount. A PC computer collected force data at 100 Hz for 25 s with the 12-bit analog-to-digital converter. Drag at each velocity was calculated as the average of the 2500 points collected at each velocity. The algae were positioned upside down in the tank to keep the force transducer dry; while this posture may have influenced the alga's shape and projected area of alga at very low velocities (<0.1 m s^{-1}), gravitational and buoyant forces were otherwise negligible. Further references to the position and orientation of an alga reflect the natural, upright perspective, despite the experimental conditions.

To compare to previous studies, Vogel's E was calculated as the slope of the log–log plot of speed-specific drag (F_D/U^2) *versus* velocity (Vogel, 1994). Due to the broad range of water velocities examined and the differences between low velocity and high velocity reconfiguration, E was determined for two separate velocity ranges, 0–0.5 and 0.5–2.0 m s^{-1} (Vogel, 1994). Additionally, planform area-based drag coefficients ($C_{D,plan}$) were calculated at 0.5 and 1.9 m s^{-1} (just below the maximum flow of the tank) as:

$$C_D \equiv \frac{2F_D}{\rho U^2 A}, \quad (3)$$

where the planform area was used as the characteristic area (A). Predicted force at 1.9 m s^{-1} was calculated using Eqn 2 with Vogel's E and the planform area $C_{D,plan}$ from both low velocity and high velocity ranges. A paired t-test was used to examine the difference between the predicted and measured force.

Reconfiguration was measured directly by using a two-camera high-speed digital video system to record the frontal (projected into the flow) and side views of each alga during flume runs (Fig. 1). The frontal images were obtained with a camera equipped with a 12–75 mm zoom lens pointed at an 11 cm×7 cm mirror rigidly suspended at a 45° angle in the downstream end of the diffuser (Fig. 1). Morphological data were quantified at each velocity using ImageJ software. Stipe angle, a measure of the overall posture of the alga, was defined as the angle of the stipe relative to the substrate (Fig. 2). Crown angle, a measure of the shape of the alga interacting with the flow, was defined as the angle formed by three points: the top (nearest the center of the tank) and bottom (adjacent to the wall) edges of the crown and the stipe crown junction (Fig. 2). Both stipe and crown angle were measured from the side view images.

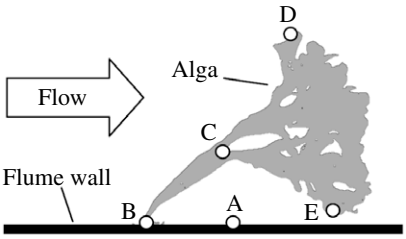

Fig. 2. Shape parameters measured directly during reconfiguration. The stipe angle was defined as the angle between the tank wall (A), the stipe/holdfast junction (B) and the center of the stipe/crown interface (C). The crown angle was defined by the upper edge of the crown (D), the center of the stipe/crown interface (C) and the lower edge of the crown (E).

Frontal area at each velocity (A_F) was measured from the frontal view images by tracing the edge of the silhouette of the alga manually in ImageJ, excluding large (>1 mm^2) gaps within the perimeter. A_F was then normalized by a representative area (A_{rep}, the frontal area when the alga was reconfigured such that the stipe was parallel to the flow at ~0.2 m s^{-1}) to remove the variation in overall size among individuals. TableCurve2D software (v4.07, Systat Software Inc., Point Richmond, CA, USA) was used to determine the best simple consensus model (a three-parameter exponential decay function) that described both individual and pooled data for velocities above 0.2 m s^{-1} (where the alga was oriented parallel with the flow). The normalized areas as a function of velocity (a_U) were then fit to the exponential decay function:

$$a_U = a_\infty + a_R e^{-U/\beta_a}, \quad (4)$$

where a_∞ is the minimum normalized area of the alga (maximum reconfiguration), a_R is a coefficient describing the magnitude of area reduced due to reconfiguration, and β_a is the normalized area reconfiguration coefficient, a term that describes the steepness of the decay function. The normalized area function parameters, goodness of fit and 95% confidence intervals were determined for both individuals and pooled data using TableCurve2D.

Velocity-specific drag coefficient was calculated using Eqn 3, where A was A_F measured directly at each specific velocity (Vogel, 1994). TableCurve2D was again used to determine the best simple model to describe the change in drag coefficient for velocities above 0.2 m s^{-1} and again an

exponential decay function was chosen. The drag coefficient as a function of water velocity (C_U) was fit to the equation:

$$C_U = C_\infty + C_R e^{-U/\beta_C}, \quad (5)$$

where C_∞ is the minimum C_D (at maximum reconfiguration), C_R is a coefficient describing the magnitude of the reduction of C_D due to reconfiguration, and β_C is the reconfiguration coefficient for C_D. The C_U function parameters and 95% confidence intervals were determined using TableCurve2D for velocities above 0.2 m s^{-1} (where the alga was oriented parallel with the flow).

Additional parameters, the critical velocities for area reconfiguration ($U_{crit,a}$) and for C_D reconfiguration ($U_{crit,C}$), were defined to express the water velocity at which reconfiguration approached its maximum effect. A threshold of within 5% of the asymptote value of Eqn 4 and 5 was chosen to represent this velocity. Because the value is approached from above, this corresponds to a value of 105% of the asymptote, thus $U_{crit,a}$ was calculated by replacing a_U with ($1.05a_\infty$) and solving for U in Eqn 4. $U_{crit,C}$ was calculated in an analogous manner. Critical values were calculated for both individual and pooled data. It should be noted that a threshold of less than 5% could have been chosen, resulting in higher U_{crit} values that were closer to the asymptote. However, lowering the threshold would result in much higher U_{crit} values with little corresponding change in the a_U or C_U because of the exponential decay.

A new model for reconfiguration

A model for drag on reconfiguring macroalgae was defined by replacing A and C_D in Eqn 1 with the pooled functions describing the *Chondrus*' change in area and C_D with velocity, a_U and C_U, respectively. Because a_U described the change in normalized area, the equation was multiplied by A_{rep} to describe the force on an individual, such that the mechanistic model of drag with reconfiguration (F_{DR}) was defined as:

$$F_{DR} = \tfrac{1}{2}\rho U^2 A_{rep} a_U C_U . \quad (6)$$

To examine the accuracy of the model, F_{DR} from 0.2 to 2.0 m s^{-1} was calculated for the individuals that had been previously examined in the flow tank and compared to the directly measured forces. A paired t-test was used to examine the difference between predicted and measured forces. Additionally, the upper and lower boundaries of drag predictions were calculated for all of the individuals in the study for water velocities ranging from 0.2 to 2 m s^{-1}.

Results

Macroalgae used in the study varied in size, with height ranging from 5 to 10 cm, A_{plan} ranging from 5.77 to 28.36 cm^2, and A_{rep} ranging from 5.59 to 23.14 cm^2 (Table 1).

Drag was variable among individuals, with F_D ranging from 0.28 to 1.48 N at 1.9 m s^{-1} (Fig. 3). Reconfiguration, as quantified by Vogel's E, ranged from –0.35 to –0.85 for low water velocity and –0.44 to –0.81 for high velocity (Table 1).

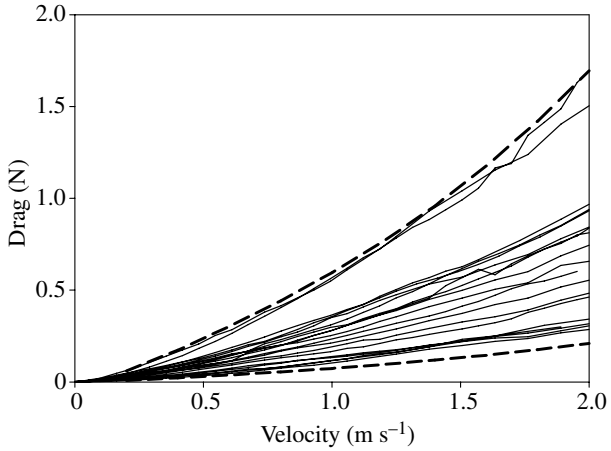

Fig. 3. Drag (F_D) on all *Chondrus* from 0 to 2 m s^{-1} water velocity. Thin lines are individual algae measured at ~0.1 m s^{-1} intervals. The broken lines are the upper and lower predicted drag for the largest and smallest individuals (based on A_{rep}) using the reconfiguration drag model (Eqn 6).

$C_{D,plan}$ calculated at 0.5 m s^{-1} ranged from 0.33 to 0.92, but was lower (0.15 to 0.46) when calculated at 1.9 m s^{-1}. The mean percent errors from the measured force were 56% for low velocity predictions and 21% for high velocity predictions (Table 1). Paired t-tests indicated significant deviation from the actual value for both low (t=–8.41, d.f.=18, P<0.01) and high (t=9.77, d.f.=18, P<0.01) velocity predictions.

Stipe angles were initially high (near 90°) in still water and dropped dramatically over low velocities, as the alga came in contact with the wall of the tank (between 0.1 and 0.2 m s^{-1}, Fig. 4). Once substrate contact was made, the stipe was held off the wall by the crown, and only gradual decreases in angle were observed as the crown compressed. Crown angles were

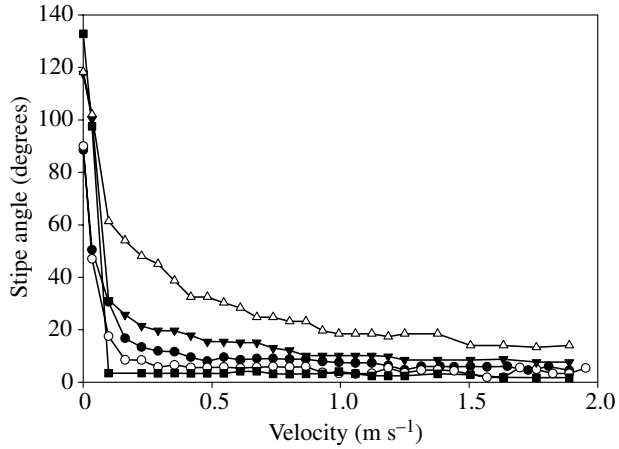

Fig. 4. Stipe angle *versus* velocity for a subset of *Chondrus* representing the range of values observed. The rapid change in angle at low velocity (<0.2 m s^{-1}) resulted in the crown contacting with the tank floor. Subsequent change in angle was due to the compression of the crown, allowing the stipe to become more parallel to the flow. Different symbols represent individual algae.

Table 1. *Morphological and hydrodynamic parameters measured for individual Chondrus*

				Low velocity model			High velocity model			
Alga	Height (cm)	A_{plan} (cm^2)	A_{rep} (cm^2)	Vogel's E	$C_{D,plan}$@ 0.5 m s^{-1}	Predicted force (N) (% error)	Vogel's E	$C_{D,plan}$@ 1.9 m s^{-1}	Predicted force (N) (% error)	Predicted F_{DR} (N) (% error)
1	8.26	20.16	13.50	–0.42	0.51	1.42 (61.67)	–0.55	0.24	0.62 (–29.33)	0.92 (4.99)
2	9.44	24.80	17.47	–0.72	0.46	1.30 (52.77)	–0.69	0.19	0.55 (–35.31)	1.19 (40.25)
3	5.98	17.98	14.25	–0.52	0.50	1.17 (37.87)	–0.44	0.26	0.65 (–24.25)	0.97 (14.11)
4	7.16	21.75	16.50	–0.72	0.49	1.23 (38.41)	–0.55	0.22	0.63 (–29.33)	1.13 (27.07)
5	6.84	9.84	6.14	–0.39	0.58	0.80 (88.41)	–0.66	0.24	0.28 (–34.07)	0.42 (–1.65)
6	6.05	20.46	12.75	–0.84	0.41	0.89 (17.45)	–0.56	0.20	0.53 (–29.78)	0.87 (15.40)
7	9.38	28.36	23.14	–0.64	0.62	2.12 (42.40)	–0.53	0.29	1.06 (–28.44)	1.58 (6.14)
8	7.84	8.01	9.49	–0.66	0.91	0.87 (51.88)	–0.59	0.40	0.40 (–31.10)	0.65 (12.78)
9	8.96	16.66	14.24	–0.85	0.57	1.00 (31.70)	–0.49	0.25	0.56 (–26.61)	0.97 (27.57)
10	5.18	9.89	6.14	–0.73	0.33	0.37 (21.93)	–0.47	0.17	0.23 (–25.67)	0.40 (28.67)
11	6.98	5.77	5.61	–0.57	0.78	0.57 (90.13)	–0.81	0.29	0.18 (–40.03)	0.38 (27.45)
12	4.98	8.86	7.06	–0.45	0.75	0.91 (75.67)	–0.66	0.32	0.34 (–34.07)	0.48 (–6.86)
13	5.21	11.36	10.22	–0.42	0.89	1.40 (79.71)	–0.65	0.38	0.52 (–33.66)	0.70 (–10.63)
14	5.18	6.11	4.45	–0.48	0.66	0.54 (83.02)	–0.75	0.27	0.18 (–37.72)	0.30 (3.32)
15	9.10	15.48	9.89	–0.74	0.41	0.73 (63.58)	–0.70	0.16	0.29 (–35.72)	0.67 (51.41)
16	8.96	10.16	5.59	–0.51	0.33	0.45 (60.04)	–0.56	0.15	0.20 (–29.78)	0.38 (36.82)
17	7.58	16.85	15.40	–0.35	0.92	2.25 (60.12)	–0.54	0.46	1.00 (–28.89)	1.05 (–25.16)
18	9.78	17.04	11.73	–0.58	0.45	0.96 (50.53)	–0.64	0.21	0.42 (–33.24)	0.80 (26.07)
19	6.74	11.36	9.37	–0.51	0.72	1.07 (56.12)	–0.56	0.33	0.48 (–29.78)	0.64 (–6.95)
Mean	7.35	14.31	11.21	–0.58	0.59	1.05 (55.97)	–0.60	0.26	0.48 (–31.41)	0.76 (14.25)
s.e.m.	0.37	1.41	1.13	0.03	0.04	0.11	0.02	0.02	0.06	0.08

Low (0–0.5 m s^{-1}) and high (0.5–2.0 m s^{-1}) velocity models refer to Vogel's E and $C_{D,plan}$ calculated at those ranges and force predicted at 1.9 m s^{-1} from those parameters using Eqn 2. F_{DR} was calculated using Eqn 6. The percent errors were calculated as percent difference between the prediction and the drag measured at 1.9 m s^{-1}.

For abbreviations, see List of symbols.

more variable than stipe angles, with changes in the position of branches causing fluctuations at low water velocities (<0.5 m s^{-1}). Angles generally decreased as velocity increased, indicating compaction of the crown (Fig. 5).

Frontal area generally decreased with water velocity for all individuals (Fig. 6). Note that A_F often increased at extremely low velocities (<0.1 m s^{-1}) as the posture of the alga changed from upright to parallel with the flow. Eqn 4 described a_U well

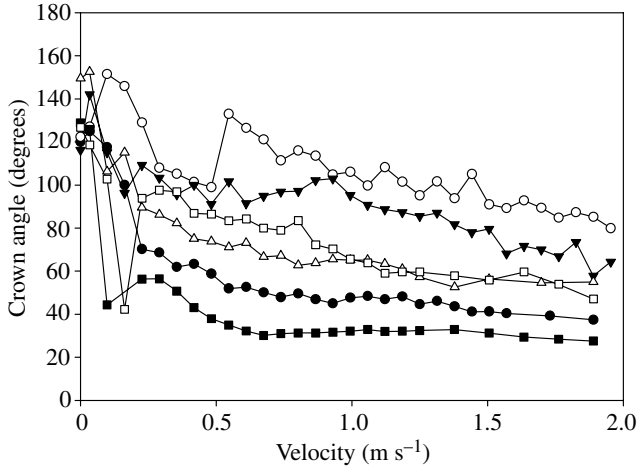

Fig. 5. Change in crown angle with velocity for a subset of *Chondrus* representing the range of values observed. Variability in angle at low velocity was due to changes in the position of branches within the crown. Subsequent changes in angle were due to the compression of the crown. Different symbols represent individual algae.

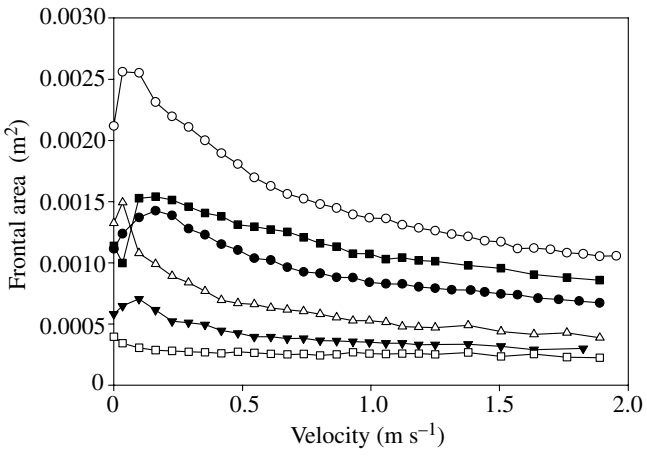

Fig. 6. Change in frontal area (A_F) with water velocity for a subset of *Chondrus* representing the range of values observed. Initial increases in area at low water velocities (<0.2 m s^{-1}) were due to an overall posture change of individuals. Subsequent decrease in area was due to crown compression. Different symbols represent individual algae.

Table 2. *Exponential decay function parameters and goodness of fit for frontal area and drag coefficient for Chondrus*

	Area					Drag coefficient				
Alga	a_∞	a_R	β_a (m s^{-1})	R^2	$U_{crit,a}$ (m s^{-1})	C_∞	C_R	β_C (m s^{-1})	R^2	$U_{crit,C}$ (m s^{-1})
1	0.51	0.72	0.68	0.98	2.27	0.74	0.82	0.59	0.91	1.83
2	0.32	0.80	0.88	0.99	3.44	0.69	0.70	0.43	0.98	1.29
3	0.46	0.74	0.61	0.99	2.12	0.70	0.89	0.25	0.96	0.81
4	0.39	0.89	0.49	0.98	1.87	0.81	1.12	0.30	0.97	1.00
5	0.36	0.83	0.73	0.99	2.80	0.89	0.74	0.54	0.94	1.52
6	0.39	0.79	0.53	0.97	1.96	0.81	0.64	0.46	0.94	1.27
7	0.42	0.78	0.72	0.99	2.60	0.75	1.01	0.33	0.98	1.09
8	0.40	0.79	0.78	0.99	2.87	0.83	1.37	0.29	0.97	1.01
9	0.41	0.76	0.69	0.99	2.49	0.72	1.68	0.24	0.98	0.92
10	0.56	0.70	0.51	0.98	1.64	0.60	0.91	0.33	0.96	1.13
11	0.42	0.76	0.78	0.99	2.80	0.55	0.98	0.76	0.99	2.72
12	0.47	0.69	0.81	0.98	2.74	0.69	0.84	0.85	0.97	2.71
13	0.49	0.70	0.61	0.99	2.04	0.81	1.02	0.71	0.94	2.29
14	0.34	0.76	1.30	0.97	4.94	0.96	0.80	0.65	0.97	1.83
15	0.42	0.80	0.61	0.98	2.22	0.62	1.27	0.37	0.98	1.37
16	0.41	0.81	0.66	0.97	2.43	0.66	0.90	0.24	0.91	0.79
17	0.46	0.67	1.04	0.99	3.51	0.90	0.67	0.54	0.95	1.46
18	0.49	0.66	0.62	0.96	2.04	0.61	0.79	0.63	0.97	2.05
19	0.56	0.66	0.54	0.99	1.71	0.64	0.77	0.82	0.97	2.61
Mean	0.44	0.75	0.72	0.98	2.55	0.74	0.94	0.49	0.96	1.56
s.e.m.	0.02	0.01	0.05		0.18	0.03	0.06	0.05		0.15

All regressions had $P<0.01$.
Parameters were estimated using TableCurve2D for velocities ranging from 0.2 to 2.0 m s^{-1}.
For abbreviations, see List of symbols.

for water velocities above 0.2 m s^{-1} (all $P<0.01$; R^2=0.96–0.99), with parameter ranges of: a_∞=0.32–0.56, a_R=0.66–0.89, and β_a=0.49 to 1.30 m s^{-1} (Table 2). The fit of pooled data was also well described by Eqn 4 ($P<0.01$, R^2=0.89) and were very similar to the means of individual fits.

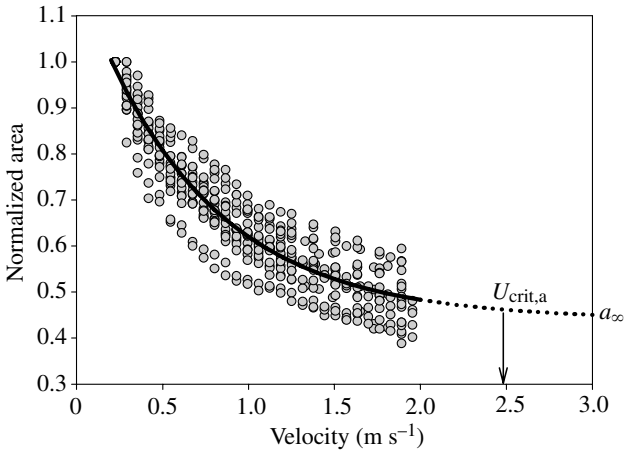

Fig. 7. Normalized area *versus* velocity for all *Chondrus*. The line is a_U, the exponential decay function describing the normalized area from 0.2 to 2.0 m s^{-1} (Eqn 4). Model parameters (±95% confidence intervals) are: a_∞=0.44±0.02, a_R=0.75±0.03, β_a=0.70±0.08 m s^{-1}; R^2=0.98. $U_{crit,a}$ (2.47 m s^{-1}) is noted by the arrow.

Pooled parameters (±95% confidence intervals) were estimated as: a_∞=0.44±0.02, a_R=0.75±0.03, and β_a=0.70±0.08 m s^{-1} (Fig. 7). Individual $U_{crit,a}$ ranged from 1.64 to 4.94 m s^{-1} and averaged 2.55 m s^{-1} (Table 2). The pooled $U_{crit,a}$ was 2.47 m s^{-1}.

Drag coefficient decreased with increasing water velocity, ranging from 1.02 to 1.57 at 0.2 m s^{-1} and 0.56 to 0.92 at 2.0 m s^{-1} (Fig. 8). Eqn 5 described C_D well for water velocities above 0.2 m s^{-1} (all $P<0.01$; R^2=0.91–0.99) with parameter ranges of C_∞=0.55–96, C_R=0.64–1.68 and β_C=0.24–0.85 m s^{-1} (Table 2). When pooled among individuals, the C_U model yielded parameters (±95% confidence intervals) of C_∞=0.75±0.03, C_R=0.87±0.12 and β_C=0.42±0.08 m s^{-1} ($P<0.01$; R^2=0.59; Fig. 8). Again, pooled parameter values were very similar to the means of individual parameters. Drag coefficient was also correlated with the shape of the crown at low to intermediate velocities (0.2–0.7 m s^{-1}). In general, C_D values increased with crown angle (mean slope=0.016, mean R^2=0.70), such that broader crowns had higher C_D values (Fig. 9). Individual $U_{crit,C}$ ranged from 0.79 to 2.72 m s^{-1} and averaged 1.56 m s^{-1} (Table 2). The pooled $U_{crit,C}$ was 1.32 m s^{-1}.

The reconfiguration drag model predicted a range of forces that encompassed all of the forces measured for the individuals in the study (Fig. 3). At 1.9 m s^{-1}, predicted drag on individuals had a mean percent error of 12% (Table 1). A paired *t*-test

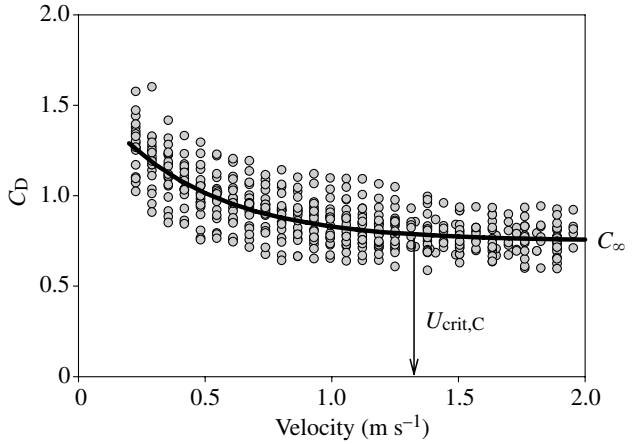

Fig. 8. Drag coefficient (C_D) *versus* water velocity for all *Chondrus*. The line is C_U, the exponential decay function describing C_D from 0.2 to 2.0 m s^{-1} (Eqn 5). Model parameters (±95% confidence intervals) are: C_∞=0.75±0.03, C_R=0.87±0.12, β_C=0.42±0.08 m s^{-1} and R^2=0.59. $U_{crit,C}$ (1.56 m s^{-1}) is noted by the arrow.

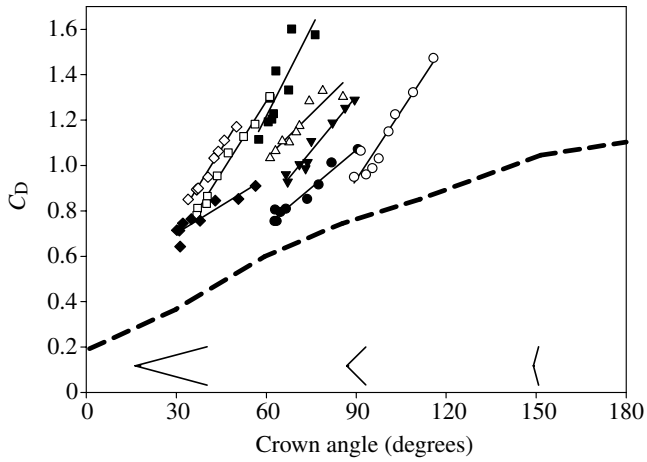

Fig. 9. Drag coefficient *versus* crown angle for representative *Chondrus* at low to intermediate water velocities (0.2 to 1.0 m s^{-1}). Reconfiguration was inversely related to crown angle such that maximal reconfiguration approaches 0°. The thin lines are linear regressions for each individual. The thick broken line was for a rigid cone of variable shape, where the cone's crown angle was equal to the angle of the peak of the cone (Hoerner, 1965). The angles above the *x*-axis represent cone of equal frontal area but spire angles of 30, 90 and 150°, respectively.

indicated a small but significant difference between predicted and measured values (t=–2.13, d.f.=18, P=0.05).

Discussion

This study is the first to measure directly changes in the size and shape of an organism as it reconfigures with increasing water velocity. These measurements permit several insights into the mechanisms of reconfiguration across a wide range of velocities, the relative importance of size and shape changes to reconfiguration, and allow for the development of a mechanistic model of drag generation for flexible macroalgae.

Low versus high velocity reconfiguration

Two distinct processes of reconfiguration are evident in this study, supporting the idea that reconfiguration across broad ranges of fluid velocity may have different mechanisms and should not necessarily be examined as a single process (Vogel, 1994). First, at low water velocities (<0.2 m s^{-1}, Fig. 4), reconfiguration is dominated by the deflection of the stipe. This 'realignment' changes the posture of the macroalga from an upright (tree-like) shape to one where the stipe is bent parallel to the flow and the overall shape is similar to a cone tethered at its peak. This realignment of the stipe causes it to be loaded in tension, rather than in bending, and should result in overall lower stresses compared to bending (Koehl, 1979). The second process of reconfiguration occurs at higher water velocities, as the crown of the alga 'compacts' and causes a gradual change in the shape (crown angle) and size (A_F) interacting with the flow (Figs 5, 6). Thus, compaction effects changes in size and shape, but not the overall posture of the alga. The different velocity ranges over which these two mechanisms of reconfiguration act highlight the pitfalls in applying low-velocity hydrodynamic data to high-velocity field conditions (Bell, 1999; Denny and Gaylord, 2002).

The two distinct mechanisms for reconfiguration have different ecological implications. Realignment in response to the oscillatory flow typical of the intertidal zone (Denny, 1988) may increase photosynthetic rates by allowing alternate sides of the alga to be exposed to light. Such posture changes may also reduce self shading (Koehl and Alberte, 1988) and light competition among individuals in an algal canopy (Greene and Gerard, 1990; Kübler and Raven, 1994). At higher velocities, where forces approach those required to dislodge individuals in the field (Carrington et al., 2001), greater compression results in lower drag. Thus greater reconfiguration by this mechanism should improve survival at higher water velocities and the preservation of photosynthetic and reproductive tissues. However, photosynthetic rates are reduced in small macroalgae across this velocity range (Stewart and Carpenter, 2003), suggesting that crown compression can negatively influence photosynthesis due to the reduction in the presentation of photosynthetic area to sunlight.

Frontal area

The two mechanisms of reconfiguration suggest that there should be little correspondence between changes in area during realignment and compaction. Realignment is effectively a change from a side view to the top view of the alga, with respect to the flow. This change in posture accounts for the unpredictable changes in frontal area at low velocities. During compaction, the change in frontal area was remarkably smooth. Additionally, there was no relationship between size (A_{plan}, A_{rep} or height) and proportion of area reduced; all individuals had relatively similar proportional decreases in frontal area, as quantified by a_∞, despite the broad range in size and bushiness

among individuals. While bushier individuals might be expected to have more potential for reconfiguration because of their three-dimensional structure, and thus have a lower a_∞, this was not the case in *Chondrus*. Further study of other macroalga shapes is warranted.

Drag coefficient

The direct measurement of area projected into the flow also allows for the calculation of drag coefficients that are comparable to those measured for rigid objects (where C_D is defined relative to frontal area). Calculated in this way, drag coefficients for *Chondrus* are similar to those of bluff bodies, i.e. non-streamlined, rigid objects with C_D>0.5 (Hoerner, 1965; Vogel, 1994). The results reported here are distinct from other macroalgae studies in which C_D is calculated with the planform area. Because C_D is inversely proportional to area (Eqn 3) and the planform area is a fixed value that is much larger than the reconfigured frontal area of a macroalga, the C_D values calculated using planform area are lower than values calculated using the reconfigured frontal area. Thus, the low C_D values reported for reconfigured macroalgae, e.g. 0.02–0.36 (Carrington, 1990), incorporate both changes in the frontal area and C_D. These planform area-calculated C_D values of reconfigured macroalgae should not be compared to those of rigid objects (see Gaylord et al., 1994; Sand-Jensen, 2003) because the two C_D values have been defined differently.

Drag coefficient did decrease across moderate water velocities, corresponding to the change in the angle of the crown (Fig. 9), such that the hydrodynamic behavior of the alga is similar to rigid cones of variable shape pointed into the flow (smaller angles resulted in lower C_D) (Hoerner, 1965). This suggests that changes in the shape of the macroalga at these velocities do result in reduced drag. At higher velocities, when C_D approaches its asymptote, the effects of shape change are greatly reduced, and the macroalga behaves more like a bluff body (high, constant C_D).

While the changes observed in drag coefficient in this study are in part attributed to the change in shape of the alga, other factors may be involved. For bluff, rigid bodies, drag coefficient is not constant across large ranges in Reynolds number (*Re*) (Vogel, 1994), thus the change in C_D observed here at low velocities may in part be due to this relationship between C_D and *Re*. However, *Re* for these macroalgae ranged from 15 000 to 150 000, a range similar to where C_D does not vary for bluff bodies (Vogel, 1994). It is also possible that the juxtaposition of the substrate to the reconfigured alga at high velocity may influence drag through an interaction with the boundary layer (Vogel, 1994). The flow in the flume was turbulent, suggesting that high velocities extended very near to the substrate (Denny, 1988). Carrington measured velocities in a similar flume that were ~70% of the free stream flow within ~2 mm from the substrate at a free stream velocity of 1.18 m s^{-1} (Carrington, 1990). Because even small reconfigured *Chondrus* extend over 1.5 cm above the wall of the flume during maximum reconfiguration, they cannot completely hide in the boundary layer and any effect is likely small. Additionally, reconfiguration may reduce the surface area over which skin drag can occur as the flume wall shelters one side of the alga from interacting with the flow (Koehl, 1984). However, this form of drag reduction may be most applicable to blade-like species.

Shape or size

The relative contributions of area and drag coefficient to reconfiguration change with water velocity. At low to intermediate velocities, both area and C_D decrease, suggesting that both are contributing to drag reduction (Figs 7, 8). Between the $U_{crit,C}$ and $U_{crit,a}$ (1.32 and 2.47 m s^{-1}), the change in area continues while C_D has effectively reached its asymptote. Within this range, the change in area is largely responsible for drag reduction. Above both critical velocities (>2.5 m s^{-1}) both variables are predicted to be constant such that these flexible organisms behave like rigid, bluff bodies. These observations provide a mechanistic explanation to support the model proposed (Bell, 1999), where the effects of reconfiguration were limited to low velocities. Further study of drag and reconfiguration at the higher velocities seen in the field (>10 m s^{-1}) (O'Donnell, 2006) is needed to verify this hypothesis.

Should reconfiguration be considered a streamlining mechanism? In an engineering sense, streamlining is typically considered to be a process that results in reduced drag coefficient, but the term can also refer to any process that reduces drag. Algal reconfiguration does indeed reduce drag and, in a broader sense, can be considered a 'streamlining' process. It is important to note that this streamlining is accomplished mostly by reducing frontal area, not drag coefficient. However, while reconfiguration effects some reduction in C_D, the values calculated here are similar to those of bluff bodies. Thus these macroalgae do not form shapes that are 'streamlined'.

Reconfiguration drag model

The reconfiguration drag model (Eqn 6) proposed here uses measured relationships between water velocity and both frontal area and drag coefficient to predict drag. The pooled parameters describing the change in area and C_D using Eqn 4 and 5, respectively, are representative of the population of *Chondrus* examined in the study and are meant to broadly describe the hydrodynamic performance of the *Chondrus* morphologies found in the wave-swept intertidal zone. Thus, the pooled parameters include error due to the morphological variation among individuals and are probably best applied at a population level, not an individual level. Nonetheless, the pooled model predictions for individuals are all within 0.4 N at 2.0 m s^{-1} (Table 1). Examination of individual variation would necessitate comparisons of the model fit to individuals' data.

The use of a mechanistic model for drag generation on a flexible organism improves our ability to predict drag at higher, ecologically relevant water velocities. Due to the complexity of drag generation and the variety of mechanisms that can contribute to reconfiguration, it has been unclear how to

extrapolate low velocity patterns to the velocities that would produce large enough forces to damage and remove individuals (Bell, 1999). This problem is exacerbated by the fact that most studies of reconfiguration are limited to low water velocities (<1.0 m s^{-1}), due to the limitations of flume design, and the difficulty of directly measuring drag in the field. In this study, predictions of drag using Vogel's E and the planform area calculated at low and high velocities consistently overestimate and underestimate drag at a higher velocity, respectively. Our proposed model had a smaller but still significantly different deviation from the measured force. However, the asymptotic decline in a_U and C_U suggests that the macroalgae will behave more as bluff bodies at high water velocity, allowing for more accurate extrapolation to higher water velocities. For example, in this study, $U_{crit,a}$ is extrapolated to be 2.47 m s^{-1}, and is calculated as 2.76 in another study with a larger range of velocities (up to 3.0 m s^{-1}) (M. L. Boller and E. Carrington, manuscript submitted for publication). This suggests that medium velocity measurements (in the range of 3 m s^{-1}) may be sufficient to make drag predictions for some macroalgae, precluding the need to make difficult high-velocity drag measurements. However, high velocity tests of this model are needed.

The reconfiguration drag model also provides variables that can be used to compare the hydrodynamic performance of macroalgal species and reconfiguring marine invertebrates. Variation in $U_{crit,a}$ and $U_{crit,C}$ among species represents differences in the rate of reconfiguration relative to water velocity, while differences in a_∞ and C_∞ are indicative of variation in the absolute magnitude of reconfiguration. With these measures of hydrodynamic performance, it may be possible to relate the effects of morphological and material property variation to ecological performance.

The reconfiguration drag model (Eqn 6) may be considered more complicated than the Vogel's E-corrected drag equation (Eqn 2) or others proposed to describe drag on flexible organisms (e.g. Gaylord, 2000; Denny and Gaylord, 2002) because of the addition of functions that describe area and C_D changes with velocity (Eqn 4 and 5). However, these parameters are necessary to quantify the changes in the representative area and C_D because of the shape of the curve (an exponential decay) and because the values do not asymptote to zero. However, the proposed model could be considered less complicated because it preserves the standard relationship between drag and flow velocity (i.e. $F_D \propto U^2$). .

Conclusions

The reconfiguration of macroalgae is an unavoidable consequence of their flexibility and an essential component for their strategy for survival in the wave-swept rocky intertidal zone (Denny and Gaylord, 2002; Harder et al., 2004). This study clarifies the mechanisms by which reconfiguration reduces drag: realignment and crown compaction. The latter process reduces frontal area and drag coefficient of the macroalga by changing the shape of the crown. These data reinforce the hypothesis that reconfiguration is a dynamic process influenced by velocity-dependent mechanisms (Vogel, 1994) and suggests that reconfiguration in *Chondrus* is dominated by a change in size of the macroalga and is less influenced by the interaction between the macroalga's shape and the flow. The mechanistic model proposed here provides a method of predicting drag on a flexible organism based on the predictable changes in area and C_D with water velocity. Because it is based on the mechanisms underlying reconfiguration, it improves our ability to predict drag on flexible organisms at high, ecologically relevant water velocities above the limits of a flume. Most importantly, it provides a framework to (1) compare the hydrodynamic performance among flexible organisms and (2) investigate physical characteristics of the organisms that may influence their hydrodynamic and ecological performances.

List of symbols

a_∞	minimum normalized area
a_R	normalized area reduced due to reconfiguration
a_U	normalized area as a function of velocity
A	characteristic area
A_F	frontal area
A_{plan}	planform area
A_{rep}	representative area at low reconfiguration
β_a	reconfiguration coefficient of normalized area
β_C	reconfiguration coefficient of the drag coefficient
C_D	drag coefficient
$C_{D,plan}$	planform area drag coefficient
C_∞	minimum drag coefficient
C_R	drag coefficient reduced due to reconfiguration
C_U	drag coefficient as a function of velocity
E	Vogel's E
F_D	drag
F_{DR}	drag of reconfiguration
ρ	fluid density
U	velocity of the fluid relative to the organism
$U_{crit,a}$	critical velocity of area reconfiguration
$U_{crit,C}$	critical velocity of C_D reconfiguration

C. Wilga, J. Hetshe, G. Moeser, P. Martone, L. Hunt, M. Denny, A. Johnson and an anonymous reviewer provided helpful comments and discussion on this manuscript. J. Sylvester and H. Vargas provided assistance in the laboratory, and C. Wilga afforded the use of the high-speed cameras. This work was supported financially by donations from Mike Pace and Anadarko Petroleum and a URI Foundation Grant Fellowship to M.L.B., NSF OCE-0082605.

References

Bell, E. C. (1999). Applying flow tank measurements to the surf zone: predicting dislodgment of the Gigartinaceae. *Phycol. Res.* **47**, 159-166.

Carrington, E. (1990). Drag and dislodgment of an intertidal macroalga: consequences of morphological variation in *Mastocarpus papillatus* Kützing. *J. Exp. Mar. Biol. Ecol.* **139**, 185-200.

Carrington, E. (2002). Seasonal variation in the attachment strength of blue mussels: cause and consequences. *Limnol. Oceanogr.* **47**, 1723-1733.

Carrington, E., Grace, S. P. and Chopin, T. (2001). Life history phase and the biomechanical properties of the red alga *Chondrus crispus* (Rhodophyta). *J. Phycol.* **37**, 699-704.

Dayton, P. K. (1971). Competition, disturbance, and community organization: the provision and subsequent utilization of space in a rocky intertidal community. *Ecol. Monogr.* **41**, 351-389.

Denny, M. W. (1988). *Biology and Mechanics of the Wave Swept Environment.* Princeton: Princeton University Press.

Denny, M. W. (1995). Predicting physical disturbance: mechanistic approaches to the study of survivorship on wave-swept shores. *Ecol. Monogr.* **65**, 371-418.

Denny, M. W. and Gaylord, B. P. (2002). The mechanics of wave-swept algae. *J. Exp. Biol.* **205**, 1355-1362.

Denny, M. and Wethey, D. (2001). Physical processes that generate patterns in marine communities. In *Marine Community Ecology* (ed. M. D. Bertness, S. D. Gains and M. E. Hay), pp. 3-37. Cambridge: Cambridge University Press.

Denny, M. W., Daniel, T. L. and Koehl, M. A. R. (1985). Mechanical limits to size in wave-swept organisms. *Ecol. Monogr.* **55**, 69-102.

Denny, M. W., Gaylord, B. P. and Cowen, E. A. (1997). Flow and flexibility. II. The roles of size and shape in determining wave forces on the bull kelp *Nereocystis luetkeana. J. Exp. Biol.* **200**, 3165-3183.

Garbary, D. J. and DeWreede, R. E. (1988). Life history phases in natural populations of Gigartinaceae (Rhodophyta): quantification using resorcinol. In *Experimental Phycology* (ed. C. S. Lobban, D. J. Chapmin and B. P. Kramer), pp. 174-178. Cambridge: Cambridge University Press.

Gaylord, B. (2000). Biological implications of surf zone complexity. *Limnol. Oceanogr.* **45**, 174-188.

Gaylord, B. P. and Denny, M. W. (1997). Flow and flexibility. I. Effects of size, shape and stiffness in determining wave forces on the stipitate kelps *Eisenia arborea* and *Pterygophora californica. J. Exp. Biol.* **200**, 3141-3164.

Gaylord, B. P., Blanchette, C. A. and Denny, M. W. (1994). Mechanical consequences of size in wave-swept algae. *Ecol. Monogr.* **64**, 287-313.

Greene, R. M. and Gerard, V. A. (1990). Effects of high-frequency ligh fluctuations on growth and photoacclimation of the red alga *Chondrus crispus*. *Mar. Biol.* **104**, 337-344.

Harder, D. L., Speck, O., Hurd, C. L. and Speck, T. (2004). Reconfiguration as a prerequisite for survival in highly unstable flow dominated habitats. *J. Plant. Growth. Regul.* **23**, 98-107.

Hoerner, S. F. (1965). *Fluid-dynamic Drag*. Brick Town, NJ: Published by the author.

Johnson, A. S. (2001). Drag, drafting, and mechanical interactions in canopies of the red alga *Chondrus crispus*. *Biol. Bull.* **201**, 126-135.

Koehl, M. A. R. (1977). Effects of sea anemones on the flow forces they encounter. *J. Exp. Biol.* **69**, 87-105.

Koehl, M. A. R. (1979). Stiffness or extensibility of intertidal algae: a comparative study of modes of withstanding wave action. *J. Biomech.* **12**, 634.

Koehl, M. A. R. (1984). How do benthic organisms withstand moving water? *Am. Zool.* **24**, 57-70.

Koehl, M. A. R. (1986). Seaweeds in moving water: form and mechanical function. In *On the Economy of Plant Form and Function* (ed. T. J. Givnish), pp. 603-634. Cambridge: Cambridge University Press.

Koehl, M. A. R. (1999). Ecological biomechanics of benthic organisms: life history, mechanical design and temporal patterns of mechanical stress. *J. Exp. Biol.* **202**, 3469-3476.

Koehl, M. A. R. and Alberte, R. S. (1988). Flow, flapping and photosynthesis of *Nereocystis luetkeana*: a functional comparison of undulate and flat blade morphologies. *Mar. Biol.* **99**, 435-444.

Kübler, J. E. and Raven, J. A. (1994). Consequences of light limitation for carbon acquisition in three rhodophytes. *Mar. Ecol. Prog. Ser.* **110**, 203-209.

Menge, B. A. (1976). Organization of the New England rocky intertidal community: role of predation, competition, and environmental heterogeneity. *Ecol. Monogr.* **46**, 355-393.

O'Donnell, M. J. (2006). Habitats and hydrodynamics on wave-swept rocky shores. Ph.D. thesis. Stanford University, CA, USA.

Paine, R. T. and Levin, S. A. (1981). Intertidal landscapes: disturbance and the dynamics of pattern. *Ecol. Monogr.* **51**, 145-178.

Pratt, M. C. and Johnson, A. S. (2002). Strength, drag, and dislodgement of two competing intertidal algae from two wave exposures and four seasons. *J. Exp. Mar. Biol. Ecol.* **22**, 71-101.

Sand-Jensen, K. (2003). Drag and reconfiguration of freshwater macrophytes. *Freshw. Biol.* **48**, 271-283.

Sand-Jensen, K. (2005). Aquatic plants are open flexible structures – a reply to Sukhodolov. *Freshw. Biol.* **50**, 196-198.

Sheath, R. G. and Hambrook, J. A. (1988). Mechanical adaptations to flow in freshwater red algae. *J. Phycol.* **24**, 107-111.

Stewart, H. L. (2004). Hydrodynamic consequences of maintaining an upright posture by different magnitudes of stiffness and buoyancy in the tropical alga *Turbinaria ornata. J. Mar. Sys.* **49**, 157-167.

Stewart, H. L. and Carpenter, R. C. (2003). The effects of morphology and water flow on photosynthesis of marine macroalgae. *Ecology* **84**, 2999-3012.

Sukhodolov, A. (2005). Comment on drag and reconfiguration of macrophytes. *Freshw. Biol.* **50**, 194-195.

Vogel, S. (1984). Drag and flexibility in sessile organisms. *Am. Zool.* **24**, 37-44.

Vogel, S. (1989). Drag and reconfiguration of broad leaves in high winds. *J. Exp. Bot.* **40**, 941-948.

Vogel, S. (1994). *Life in Moving Fluids* (2nd edn). Princeton: Princeton University Press.